

# The distribution of absorbing column densities among Seyfert 2 galaxies

G. Risaliti

Dipartimento di Astronomia e Scienza dello Spazio, Università di Firenze, L. E. Fermi 5, I-50125,  
Firenze, Italy

R. Maiolino and M. Salvati

Osservatorio Astrofisico di Arcetri, L. E. Fermi 5, I-50125 Firenze, Italy

## ABSTRACT

We use hard X-ray data for an “optimal” sample of Seyfert 2 galaxies to derive the distribution of the gaseous absorbing column densities among obscured active nuclei in the local Universe. Of all Seyfert 2 galaxies in the sample, 75% are heavily obscured ( $N_H > 10^{23} \text{cm}^{-2}$ ) and about half are Compton thick ( $N_H > 10^{24} \text{cm}^{-2}$ ). Intermediate type 1.8–1.9 Seyferts are characterized by an average  $N_H$  much lower than “strict” Seyfert 2s. No correlation is found between  $N_H$  and the intrinsic luminosity of the nuclear source. This  $N_H$  distribution has important consequences for the synthesis of the cosmic X-ray background. Also, the large fraction of Compton thick objects implies that most of the obscuring gas is located within a radius of a few 10 pc from the nucleus.

*Subject headings:* Galaxies: active — Galaxies: nuclei — Galaxies: Seyfert — X-rays: galaxies

## 1. Introduction

According to the so-called unified model (Antonucci 1993) the same engine is at work in all Active Galactic Nuclei (AGNs). The differences between type 1 and type 2 AGNs are ascribed solely to orientation effects: our line of sight to the nucleus may (type 2) or may not (type 1) be obstructed by optically thick material, perhaps distributed in a toroidal geometry. The knowledge of the amount of obscuring gas in Seyfert galaxies is important to understand the physical properties and the nature of the putative torus, but is also relevant to other AGN-related issues, such as the cosmic X-ray background. Indeed, the distribution of the absorbing  $N_H$  is a key ingredient in background synthesis models (Comastri et al. 1995, Gilli et al. 1999a).

When the photoelectric absorption cutoff is observed in the hard X-ray spectrum of a given source, the column density of the obscuring gas is easily measured, at least in principle. In the spectral analysis of these sources an extra emission at low energies is often present, the so-called

“soft excess” (ascribed either to scattered radiation or to diffuse thermal emission), which is fitted with a separate model component. The  $N_H$  which is derived from the fit is the one that obscures the central emission of the AGN, while other opacities affecting the reflected or diffuse radiation are not relevant in the present context. When instead only a reflected component is visible, and the direct component is completely suppressed in the observed spectral range, one can deduce only a lower limit for  $N_H$ , which depends on the maximum energy for which measurements are available (for a detailed discussion see Maiolino et al. 1998a, hereafter M98).

Many Seyfert 2s (hereafter Sy2s) were observed in the past by various X-ray satellites such as Einstein, Ginga and, more recently, ASCA, ROSAT, and BeppoSAX. The main limitation of previous studies on the  $N_H$  distribution of Sy2s was the strong bias in favor of X-ray bright sources, which tend to be the least absorbed ones. However, recent observations have probed X-ray weaker Sy2s, partly removing the selection against heavily obscured objects (Salvati et al. 1997, Awaki et al. 1997, M98, Risaliti et al. 1999). Several works have tackled the issue of the  $N_H$  distribution by taking advantage of these new data. M98 compare the  $N_H$  distribution of past surveys with that obtained from the BeppoSAX survey of an [OIII]–selected Sy2 sample, and emphasize the bias against heavily absorbed objects in the former. Bassani et al. (1999, hereafter B99) present the  $N_H$  distribution of the whole sample of Sy2s for which hard X-ray data are available, and of an optically selected subsample. All of these works are still affected by selection effects or by incompleteness problems; they are nonetheless useful to monitor how the selection criteria can affect the shape of the  $N_H$  distribution.

Here we start from an optical sample of Seyfert 2 galaxies which is the best available one in terms of biases related to absorption. From it we extract a nuclear–flux limited subsample for which almost complete hard X-ray information exists, either published, or produced by us from archival data. The absorbing column density distribution is derived from this “optimal” subsample. In Section 2 we describe the selection criteria of the subsample, and discuss the correction of residual biases and incompleteness effects. In Section 3 we present the  $N_H$  distribution which is obtained, and briefly analyze the physical consequences of our results.

## 2. Sample selection.

In this paper with the name “Seyfert 2” we refer to sources classified as type 1.8, 1.9, and 2 in optical catalogs. Our “parent” sample of Seyfert 2 galaxies is that of Maiolino & Rieke (1995, hereafter MR), completed with NGC 1808<sup>1</sup>. We also consider 18 new Seyferts found by Ho et al. (1997), which would have been included in MR if they had been discovered earlier. These 18 additional sources are useful in order to test MR in terms of completeness and residual biases, as will become clear in the following; however, none of them will be included in the

---

<sup>1</sup>This source fits the selection criteria of Maiolino & Rieke, but was missed by the original version of the sample.

final subsample (because of the selection criteria of the latter), and we do not have to tackle problems related to possible dishomogeneities between MR and Ho et al. The MR Seyferts are identified spectroscopically within the Revised Shapley Ames catalog of galaxies (RSA, Sandage & Tammann 1987), which is limited in the B magnitude of the host galaxy ( $B_T < 13.4$  mag). Ho et al. (1997) select their Seyfert galaxies with the same criterion, but they cut the RSA to a lower limiting magnitude ( $B_T < 12.5$  mag) and require that  $\delta > 0^\circ$ ; on the other hand, they generally have spectra with higher signal-to-noise. Hard X-ray spectra are available for 43 of the MR Sy2s and for 1 out of the 18 additional sources of Ho et al. The naive approach of taking the  $N_H$  distribution of these 44 objects cannot be adopted, however, because of possible residual biases and incompleteness problems. We discuss these issues in the following.

As mentioned in the Introduction, a large fraction of the Sy2s with hard X-ray spectra were observed because they were known to be bright according to all-sky X-ray surveys, and very likely this selection criterion introduced a bias in favor of little absorbed objects (see M98 for a detailed discussion). A Sy2s (sub)sample suitable for determining a more reliable distribution of  $N_H$  should be selected according to criteria independent of absorption effects. The optimal sample should be limited in the *intrinsic flux* (i.e. before absorption) of the active nucleus.

A good indicator of the intrinsic AGN flux is the intensity of the [OIII]  $\lambda 5007$  Å emission line that is produced in the Narrow Line Region (NLR) on the 100-pc scale and, therefore, is little affected by the nuclear obscuration on the pc scale. However, MR showed that the host galaxy gaseous disk might obscure part of the NLR (see also di Serego Alighieri et al. 1997 and Hes et al. 1993), and it is important to correct the [OIII] flux for large scale absorption. The magnitude of the correction can be derived from the (narrow line) Balmer decrement. According to the unified model, the ratio between the *observed* and the *intrinsic* X-ray luminosity of a Seyfert nucleus is a measure of the absorbing  $N_H$  along the line of sight. Therefore, if the (extinction corrected) [OIII] luminosity is proportional to the intrinsic luminosity, then an estimate of  $N_H$  is provided by the ratio between the observed X-ray flux and the corrected [OIII] flux. The expected relation was confirmed and calibrated by a recent statistical study on a large sample of Seyfert 2 galaxies (B99).

In Table 1 we report the MR sample in order of decreasing absorption-corrected [OIII] flux, while in Table 2 we report the 18 additional sources from the Ho et al. sample. All data are taken from the literature, with the exception of 5 objects (NGC 4565, NGC 5005, IC 2560, NGC 5347, and IC 5135), which have been observed but whose hard X-ray data have not been published yet. For these sources, we have retrieved and analyzed the data from the ASCA public archive. The results of our analysis are briefly summarized in the Appendix. NGC 4945 and IC 2560 do not have [OIII] data, but their [OIII] flux is inferred to be quite high based on their X-ray flux (see the Appendix for more details). As discussed above, most of the sources in Table 1 were selected for hard X-ray observation because they were found bright in previous all-sky X-ray surveys. Only 13 of them were selected because of their strong [OIII] flux ( $> 40 \times 10^{-14}$  erg cm $^{-2}$  s $^{-1}$ ) without a previous X-ray survey detection (Salvati et al. 1997, M98, Risaliti et al. 1999, Awaki et al.

1997). The  $N_H$  distribution of the latter set is strongly biased towards high values of  $N_H$  (M98), as expected, since their non-detection in X-ray surveys, and their high intrinsic flux implied by the [OIII] can be reconciled only by a strong pc-scale absorption.

We now note that Table 1 has 9 sources with “high” [OIII] flux ( $> 40 \times 10^{-14}$  erg s $^{-1}$  cm $^{-2}$ ) and with no hard X-ray data, or with a signal-to-noise not good enough to provide spectroscopic information<sup>2</sup>. To all these 9 sources one can apply the same line of reasoning of the 13 [OIII]–selected sources mentioned above, and one can plausibly assume that both sets have the same distribution of column densities.

The 18 additional sources discovered in the RSA by Ho et al. (1997) have systematically low [OIII] fluxes ( $F_{[OIII]} = 33 \times 10^{-14}$  erg s $^{-1}$  cm $^{-2}$  for the brightest one, the others have  $F_{[OIII]} < 20 \times 10^{-14}$  erg cm $^{-2}$ s $^{-1}$ ): they are intrinsically weak, in accordance with their being unnoticed until recently in the optical. These new additions to the original MR sample are evidence that the latter is incomplete at low [OIII] fluxes, and the incompleteness could entail a bias in favor of low absorption in low luminosity objects. This would be analogous to the bias that affected older optically selected Seyfert samples which indeed, as shown by MR, avoided low luminosity, highly obscured AGNs. The same bias might show up here, since these faint nuclei are in any case difficult to detect and a substantial absorption could take them below the detection limit.

Hints of this effect at low fluxes come from the comparison of the  $N_H$  values of the  $F_{[OIII]} > 40 \times 10^{-14}$  erg cm $^{-2}$  s $^{-1}$  subsample with the one having  $3 \times 10^{-14}$  erg cm $^{-2}$  s $^{-1} < F_{[OIII]} < 40 \times 10^{-14}$  erg cm $^{-2}$ s $^{-1}$  (there are no X-ray data for sources with  $F_{[OIII]} < 3 \times 10^{-14}$  erg cm $^{-2}$ s $^{-1}$ ; here, only in order to compare high and low flux sources, we merge together Tabs. 1 and 2). Out of the 45 brightest Sy2s only 2 objects (i.e. 5%) have  $N_H < 10^{22}$  cm $^{-2}$ , while among the next fainter 27 at least 6 (i.e. 22%) have such a low  $N_H$ . Assuming that the true distribution is given by the first set, there is already a  $2\sigma$  excess of low absorption objects in the second set, notwithstanding the large incompleteness of its hard X-ray data.

Alternately, the differences between the two  $N_H$  distributions could arise because of a real physical dependence of the column density on the intrinsic luminosity of the source. In order to explore this hypothesis, we looked for a correlation between  $N_H$  and [OIII] luminosity among the 45 strongest [OIII] sources, and found none (upper panel of Fig. 1). The same result (i.e. no correlation) is found by comparing the  $N_H$  distribution directly with the absorption corrected X-ray (2–10 keV) luminosity<sup>3</sup>, as shown in the lower panel of Fig. 1.

Further evidence for a bias affecting the [OIII]–faint nuclei comes from the axial ratios (a/b)

---

<sup>2</sup>This is the case of NGC 1667, which shows a decreasing flux in a timescale of years, so that the  $N_H$  is unknown (see B99 for more details).

<sup>3</sup>This can be done only for objects whose X-ray spectrum shows the direct transmitted component, not for those which are completely Compton thick.

of the host galaxies (Fig. 2): the faintest [OIII] sources are seen preferentially face-on, while the brightest ones have an isotropic distribution for  $a/b > 0.2$  (axial ratios lower than 0.2 are difficult to find because of the galactic disk thickness). The reason is probably that faint AGNs are hardly detected if the host galaxy is edge-on, since then the NLR emission is partially absorbed. This result further supports the idea that the subsample of faint objects is biased in terms of obscuration. To prevent our results from being affected by the same bias, we excluded from our study all the objects with an [OIII] flux less than  $40 \times 10^{-14} \text{ erg cm}^{-2}\text{s}^{-1}$ . This selection criterion automatically excludes all the additional sources from the Ho et al. sample; this is illustrated in Fig. 3 where the [OIII] flux distribution is shown.

With the sample selection discussed above, we do not use all the available data (8 of the ignored objects have X-ray spectra: 18% of the total), but we can assume that the remaining 45 objects constitute the least biased subsample now available.

A final concern regards the optical classification of some of the objects in Tab. 1, that might be different depending on the reference in the literature, and might pose into question whether these objects should be included or not. Some of the discrepant classifications are simply a matter of sensitivity of the optical spectra, and affect mostly faint objects, i.e. those with low [OIII] fluxes, that we have excluded anyway. In some intermediate type Seyferts (1.8–1.9) the slit width plays a role: narrower slits tend to miss a fraction of the NLR thus turning some of the nearby Sy1.8s into Sy1.5s; conversely, missing the nucleus with the slit could cause the opposite error. To minimize this problem we adopted the classification obtained with the widest slit, as long as the signal-to-noise of the spectra were comparable. Again, most of these intermediate Seyferts with discrepant classification are in the low-[OIII] part of Tab. 1 that we have excluded. Only two of them are in the high-[OIII] subsample, namely NGC 1275 and NGC 3031 (classified as Sy1.5s by Ho et al.): these two objects have low  $N_H$ , therefore their exclusion would further shift the  $N_H$  distribution towards high values. Variability can also play a role: in objects known to be variable (e.g. NGC 2992) we adopted the classification and the  $N_H$  measurement in the high state. Finally, a few objects have line ratios at the borderline with LINERs, whose relationship with Seyfert nuclei is still matter of debate. Only one object of this category is present in the high-[OIII] subsample, namely NGC 5005. Summarizing, uncertainties in the optical classification do not affect significantly our results thanks to our [OIII]–based selection criterion: at most 3 out of the 45 objects in the final subsample might be misclassified.

### 3. The $N_H$ distribution and its implications.

Our final subsample is composed of 45 sources: we have direct  $N_H$  measurements for 36 of them, while for the remaining 9 we can make reasonable assumptions based on their “detection history” in optical and X rays (see previous Section). The results are plotted in Fig. 4, and tabulated in Table 3; the number in brackets corresponds to objects for which only a lower limit on  $N_H$  is available. Quoted errors are  $1 \sigma$ , and they are estimated by means of a Monte Carlo

simulation in two steps: first, 9  $N_H$  values are extracted at random according to the distribution of the 13 [OIII]–selected sources mentioned in Sect. 2; these are added to the 36 known values in order to obtain a 45–entry distribution. Then, 45  $N_H$  values are extracted at random according to the latter distribution. The procedure is repeated many times and the  $1\text{--}\sigma$  interval for each bin is measured.

In the hypothesis that the [OIII] flux is a good indicator of the AGN intrinsic luminosity, and that  $N_H$  is independent of luminosity, every [OIII] selected subsample should provide the same  $N_H$  distribution. We can therefore check our assumptions about the 9 objects not observed in the X rays by repeating our analysis on a smaller set, composed only by the first 30 objects in Tab. 1 with available hard X-ray data (3 sources without such data are interspersed among them, and are ignored). The new  $N_H$  distribution is in agreement, within the errors, with the one plotted in Fig. 4. Obviously the relative errors are higher, the statistics being lower, but the check confirms that our treatment of the 9 non-observed sources does not introduce new biases.

The shape of the distribution is quite different from what was assumed up to now: we obtain that  $\sim \frac{3}{4}$  of all Sy2s are heavily obscured ( $N_H > 10^{23} \text{ cm}^{-2}$ ) and about half are Compton thick ( $N_H > 10^{24} \text{ cm}^{-2}$ ). The main uncertainty still remaining is about the fraction of completely opaque sources ( $N_H > 10^{25} \text{ cm}^{-2}$ ) with respect to “translucent” objects with  $10^{24} \text{ cm}^{-2} < N_H < 10^{25} \text{ cm}^{-2}$ . In both cases the spectra are reflection dominated in the 2–10 keV band, and cannot be distinguished by ASCA or other medium X-ray satellites. The only way of identifying column densities in the interval  $10^{24} \text{ cm}^{-2} < N_H < 10^{25} \text{ cm}^{-2}$  is by means of solid scintillating detectors sensitive around 30 keV, like the PDS instrument on board BeppoSAX.

The shaded bar in Fig. 4 indicates sources with reflection dominated spectra in the 2–10 keV spectral range, but not observed at higher energies, i.e. objects for which only a lower limit of  $10^{24} \text{ cm}^{-2}$  can be set to the absorbing column density. Placing them in the  $10^{24} \text{ cm}^{-2} < N_H < 10^{25} \text{ cm}^{-2}$  bin is a conservative assumption, which minimizes the amount of absorption required; also, a substantial population in this bin is needed for the synthesis of the X-ray background (Gilli et al. 1999b). However, if we consider the objects with sensitive observations in the 10–200 keV range (mostly by BeppoSAX), an unexpected low number of sources with  $10^{24} \text{ cm}^{-2} < N_H < 10^{25} \text{ cm}^{-2}$  comes out. Up to now, 10 Seyfert 2s with  $N_H > 10^{24} \text{ cm}^{-2}$  were observed: only 2 of them have also  $N_H < 10^{25} \text{ cm}^{-2}$ , 7 have  $N_H > 10^{25} \text{ cm}^{-2}$ , while for the remaining one the estimate is controversial. Future observations, to be performed by means of BeppoSAX and the next Japanese X-ray satellite Astro-E, will make clear whether the present lack is due to statistical fluctuations or not.

As outlined previously, our sample of 45 sources is composed by type 1.8, 1.9 and 2 Seyfert galaxies, i.e. sources that generally show indications of cold absorption in excess of the Galactic value. Nevertheless, it can be interesting to consider the  $N_H$  distribution of type 2 and type 1.8–1.9 objects separately, as done in Fig. 5. The average column density of the intermediate Seyferts is clearly much lower than that of the “strict” Sy2s, in agreement with the expectations

of the model proposed by Maiolino & Rieke (1995).

The results reported here have several astrophysical implications. Present models of the cosmic X-ray background (Comastri et al. 1995, Gilli et al. 1999a) are able to reproduce the observations at energies between 2 keV and 100 keV in terms of the contribution of the AGNs (both type 1 and type 2). Among the many parameters of such models (AGN luminosity function and evolution, type 1 to type 2 ratio, components of the mean spectrum) only the ones concerning the  $N_H$  distribution were not constrained by any direct measurement until now. The inclusion of our results on the  $N_H$  distribution in the synthesis codes, together with new determinations of the X-ray luminosity function and evolution of type 1 AGNs (Miyaji et al. 1999), leads to very important conclusions on the properties of the contributors to the hard X-ray background and, specifically, on the existence of high luminosity type 2 AGNs (QSO2s), the evolution with redshift of the type 1 to type 2 ratio, and the consistency with the hard X-ray counts which are now becoming available (Giommi et al. 1998, Cagnoni et al. 1998). All these issues will be tackled in a forthcoming paper (Gilli et al. 1999b).

Our results on the distribution of the absorbing  $N_H$  has important implications also on the spatial extension of the obscuring medium. Indeed, it is not clear yet whether the obscuring gas is confined in a relatively dense circumnuclear torus (with typical radius of a few pc), or is distributed in a larger volume on the 100-pc–1-kpc scale. Obscuring material distributed on the 100-pc scales has been observed directly by means of HST images of nearby AGNs (e.g. Malkan et al. 1998); it has been inferred also from the shape of the infrared spectra (Granato et al. 1997) and from the shortage of edge-on systems in several Seyfert galaxy samples (Keel 1980, Maiolino & Rieke 1995, Simcoe et al. 1997). If we assume that the obscuring gas is distributed within a radius  $R$  from the nucleus and with a covering factor  $f$ , then the gas mass enclosed within the region is

$$\left(\frac{M_{gas}}{M_\odot}\right) \simeq 3.5 \times 10^8 \cdot f \cdot \left(\frac{N_H}{10^{24}\text{cm}^{-2}}\right) \left(\frac{R}{100\text{ pc}}\right)^2 \quad (1)$$

where  $N_H$  is the absorbing column density along the lines of sight that intersect the obscuring medium<sup>4</sup>. If we assume that the covering factor  $f$  is responsible for the observed Sy2/Sy1 ratio ( $\simeq 4$ )<sup>5</sup> and for the opening angle of the observed light cones, then  $f \sim 0.8$ . In the case of Compton thick Sy2s a radius of the obscuring region of the order of 100 pc would imply a gas mass of the order of or larger than  $10^9 M_\odot$ , that in many objects exceeds by itself the dynamical mass in the same region. One way to have the Compton thick obscuring gas extended over the 100-pc scale would be to assume that its covering factor  $f_{CT}$  is very small ( $\ll 0.1$ ). Until a few years ago, when the only known Compton thick source was NGC 1068, this possibility could have been plausible.

---

<sup>4</sup>Eq. 1 is roughly independent of the assumed geometry, unless most of the absorbing gas is distributed in a thin shell whose thickness is much smaller than its radius. As we shall see, the latter distribution is very unlikely, since the covering factor is larger than 50%, and a thin shell so much spread out would be problematic on grounds of dynamical stability and physical origin.

<sup>5</sup>Both MR and Ho et al. (1997) give Sy2/Sy1  $\approx 4$  if Sy1.8s and Sy1.9s are grouped together in the type 2 class.

However, our new results imply  $f_{CT} \sim 0.4$ . As a consequence in most AGNs the Compton thick gas must be distributed on scales significantly smaller than 100 pc. We can investigate this issue in detail in two well studied sources, Circinus and NGC 1068. Circinus has an  $N_H = 4.3 \times 10^{24} \text{cm}^{-2}$  (Matt et al. 1999), and Maiolino et al. (1998b) have mapped its dynamical mass by means of integral field spectroscopy on scales from 100 pc down to the central 10 pc. They concluded that the Compton thick gas must be contained within  $R < 20$  pc not to exceed the dynamical mass. As for NGC 1068, if the Compton thick gas ( $N_H > 10^{25} \text{cm}^{-2}$ ) were distributed over the central 200 pc then the implied gas mass ( $> 1.6 \times 10^9 M_\odot$ ) would exceed the dynamical mass by a factor larger than 3 (Thatte et al. 1997), and would exceed the gas mass estimated by means of CO observations by a factor larger than 100 (Helfer 1997). On the other hand, gas with lower column densities ( $\sim 10^{23} \text{cm}^{-2}$  or lower) could extend over the 100-pc scale.

#### 4. Summary

We combine a large number of published and archived hard X-ray data of Seyfert 2 galaxies in the Maiolino & Rieke (1995) sample, that provide information on the absorbing column density  $N_H$ . From this database we select a subsample of objects that is limited in the *intrinsic* flux of the active nucleus, as deduced from the reddening corrected [OIII] line. After correcting for a residual incompleteness, we derive the distribution of the absorbing  $N_H$  of this subsample. This can be regarded as the best approximation (to date) to the real distribution of  $N_H$  for the local population of (moderately luminous) Seyfert 2 nuclei. Statistical errors of the distribution are also derived.

The  $N_H$  distribution turns out to be quite different from previous estimates. In particular, 75% of all Sy2s in our final sample are heavily obscured ( $N_H > 10^{23} \text{cm}^{-2}$ ) and about half are Compton thick ( $N_H > 10^{24} \text{cm}^{-2}$ ).

If treated separately, intermediate type 1.8–1.9 Seyfert galaxies are characterized by an average  $N_H$  much lower than “strict” Seyfert 2s.

In previous models of the cosmic X-ray background the largest set of free parameters was contained in the  $N_H$  distribution. Our empirical distribution can now be used instead, and it is expected to pose tight constraints to these models.

The  $N_H$  distribution has also important implications on the spatial extension of the absorbing medium (the putative torus). The large fraction of Compton thick Seyfert 2s implies that most of the Compton thick gas must be located within a few 10 pc from the nucleus, in order not to exceed the dynamical mass in the central region. However, gas with low  $N_H$  could extend to larger radii (100 pc or more).

Finally, we do not find evidence for any correlation between the absorbing  $N_H$  and the intrinsic luminosity of active nuclei, over a range of luminosities spanning 3 orders of magnitude.



We are grateful to S. Ueno for providing us with information on his data in advance of publication. We thank the anonymous referee for helpful comments. This work was partially supported by the Italian Space Agency (ASI) through the grant ARS-98-116/22.

### A. Notes on individual objects

NGC 4945 and IC 2560 do not have [OIII] data, but their X-ray properties imply that the intrinsic [OIII] flux must be high based on the following considerations. NGC 4945 is one of the nearest active galaxies and is among the brightest AGNs at energies around 100 keV. The absence of [OIII] data cannot be ascribed to an intrinsic weakness of the source, but only to the very high extinction in the edge-on galactic disk, and  $F_{[OIII]} > 40 \times 10^{-14} \text{ erg s}^{-1} \text{ cm}^{-2}$  is a conservative assumption. IC 2560 has an X-ray flux of  $4.8 \times 10^{-13} \text{ erg s}^{-1} \text{ cm}^{-2}$ , and is certainly Compton thick (see below). If  $F_{[OIII]} \leq 40 \times 10^{-14} \text{ erg cm}^{-2} \text{ s}^{-1} \text{ cm}^{-2}$ , the  $F_{2-10\text{keV}}/F_{[OIII]}$  ratio would be higher than 1. On the contrary, the diagnostic diagram for Seyfert 2s in B99 strongly suggests that this ratio is significantly lower than 1 in Compton thick sources, so very likely  $F_{[OIII]} > 40 \times 10^{-14} \text{ erg s}^{-1} \text{ cm}^{-2}$ .

Finally we report the results of the data analysis of 5 Seyfert 2s taken from the ASCA public archive. All errors are at the 90% confidence level for one interesting parameter.

1. NGC 4565 has a powerlaw spectrum with spectral index  $1.9^{+0.45}_{-0.30}$  and no evidence of absorption. The 2–10 keV flux is  $1.8 \times 10^{-12} \text{ erg cm}^{-2} \text{ s}^{-1}$ . Both the spectral shape and the high X/[OIII] flux ratio ( $F_{2-10\text{keV}}/F_{[OIII]} = 30$ ) strongly suggest that this is a Compton thin source. The spectral fit constrains the  $N_H$  to be lower than  $6 \times 10^{21} \text{ cm}^{-2}$  (at a confidence level of 90%).
2. NGC 5005 shows a steep powerlaw spectrum with spectral index  $2.15^{+0.35}_{-0.30}$  and no absorption. The 2–10 keV flux is  $3 \times 10^{-13} \text{ cm}^{-2} \text{ erg s}^{-1}$  and the 6.4 keV iron  $K_\alpha$  line is not detected, but with a high upper limit on its equivalent width (900 eV). The X/[OIII] flux ratio is low ( $F_{2-10\text{keV}}/F_{[OIII]} = 0.15$ ), locating this source among the Compton thick sources in the diagram of B99. There is no evidence of a cold reflected component at high energies ( $E > 5 \text{ keV}$ ). Our interpretation is that we see only the extended starburst component of the host galaxy, while the AGN X-ray emission is fully absorbed. The absence of the reflected component may be due to orientation effects (the reflecting torus may be almost perfectly edge-on). For this reason we estimate a lower limit for the nuclear  $N_H$  of  $10^{24} \text{ cm}^{-2}$ , which is the minimum value required to absorb all the direct emission in the ASCA spectral range.
3. IC 2560 has a prominent iron line with  $\text{EW}(\text{Fe}) = 6.3^{+2.6}_{-3.0} \text{ keV}$  ( $E = 6.56^{+0.25}_{-0.15} \text{ keV}$ ) typical of a Compton thick Sy2. Since it has been observed only in the 2–10 keV band, we can only set a lower limit of  $10^{24} \text{ cm}^{-2}$  to  $N_H$ . The 2–10 keV observed flux is  $4.8 \times 10^{-13} \text{ erg s}^{-1} \text{ cm}^{-2}$ .

4. NGC 5347 is another Compton thick source, with  $\text{EW}(\text{Fe}) > 1.9 \text{ keV}$  and  $F(2\text{--}10\text{keV}) = 3.8 \times 10^{-13} \text{ erg cm}^{-2} \text{ s}^{-1}$ . Therefore, we can put a lower limit of  $10^{24} \text{ cm}^{-2}$  to  $N_H$ .
5. IC 5135 has a low signal to noise spectrum (the detection is at  $5.5\sigma$ ), from which we can only estimate the flux  $F(2\text{--}10\text{keV}) = 5.1 \times 10^{-13} \text{ erg cm}^{-2} \text{ s}^{-1}$  and a flat spectral index ( $\Gamma < 1.40$ ). The Fe  $K_\alpha$  line is detected with an equivalent width of  $1.37^{+1.2}_{-1.2} \text{ keV}$ . The low value of the photon index, the large value of the  $\text{EW}(\text{Fe})$  and the low  $X/[\text{OIII}]$  ratio ( $F_{2\text{--}10\text{keV}}/F_{[\text{OIII}]} = 0.5$ ) strongly support the idea that this is a Compton reflection dominated spectrum, so  $N_H > 10^{24} \text{ cm}^{-2}$  for this source as well.

Table 1. The MR sample of Seyfert 2 galaxies

Name	$F_{[OIII]}^{\dagger}$	$N_H^{\ddagger}$	Name	$F_{[OIII]}^{\dagger}$	$N_H^{\ddagger}$
1 NGC1068	15800	$> 10^5(a)$	38 NGC 3185	74	
2 CIRCINUS	6970	$43000^{+19000}_{-11000}(b)$	39 NGC 6221	72	
3 IRS 07145	2010	$> 10^5(a)$	40 NGC 5674	59	$700^{+280}_{-260}(a)$
4 NGC 7314	1770	$116^{+4}_{-13}(a)$	41 NGC 1320	57	
5 IRS 18325	752	$132^{+10}_{-10}(a)$	42 NGC 3281	45	$7980^{+1900}_{-1500}(a)$
6 NGC 5643	694	$> 10^5(a)$	43 NGC 3031	43	$9.4^{+0.7}_{-0.6}(a)$
7 NGC 2992	680	$69^{+33}_{-19}(a)$	44 NGC 4945	$> 40^{**}$	$40000^{+2000}_{-1200}(a)$
8 NGC 1386	655	$> 10^4(a)$	45 IC 2560	$> 40^{**}$	$> 10^4(e)$
9 IC 3639	620	$> 10^5(c)$	46 NGC 7743	40	$\uparrow$ sample limit
10 NGC 5135	614	$> 10^4(a)$	47 NGC 4501	36	
11 NGC 5506	600	$340^{+26}_{-12}(a)$	48 NGC 7496	29	
12 MKN 1066	513	$> 10^4(d)$	49 NGC 788	27	
13 NGC 7582	445	$1240^{+60}_{-80}(a)$	50 NGC 6890	25	
14 NGC 4388	374	$4200^{+600}_{-1000}(a)$	51 NGC 6300	20	
15 NGC 4941	355	$4500^{+2500}_{-1400}(a)$	52 NGC 4395	19	
16 IC 5063	353	$2400^{+200}_{-200}(a)$	53 NGC 1358	19	
17 NGC 2110	321	$289^{+21}_{-29}(a)$	54 NGC 7590	17	$< 9.2(a)$
18 NGC 3393	316	$> 10^5(a)$	55 NGC 5033	17	$8.7^{+1.7}_{-1.7}(a)$
19 NGC 1275	311	$149^{+69}_{-69}(a)$	56 NGC 7410	16	
20 NGC 2273	277	$> 10^5(a)$	57 NGC 7479	16	
21 NGC 4258	262	$1500^{+200}_{-200}(a)$	58 IRS 11215	11	
22 NGC 5194	228	$7500^{+2500}_{-2500}(a)$	59 NGC 4579	9	$4.1^{+2.7}_{-2.7}(a)$
23 NGC 3081	215	$6600^{+1800}_{-1600}(a)$	60 NGC 3147	9	$4.3^{+3.2}_{-2.7}(a)$
24 NGC 5005	202	$> 10^4(e)$	61 NGC 3786	8	
25 NGC 1667	197		62 NGC 4594	7	$55^{+41}_{-40}(a)$
26 MKN 1073	195		63 NGC 5128	6	$1000-3500(a)$
27 NGC 5728	180		64 NGC 5427	$> 6^*$	
28 NGC 4507	158	$2920^{+230}_{-230}(a)$	65 NGC 1241	$> 4^*$	
29 NGC 1365	141	$2000^{+400}_{-400}(a)$	66 NGC 7172	4	$861^{+79}_{-33}(a)$
30 NGC 1808	131	$320^{+588}_{-318}(a)$	67 NGC 2639	4	
31 NGC 4939	112	$> 10^5(a)$	68 NGC 5273	3	
32 NGC 5347	100	$> 10^4(e)$	69 NGC 1433	2	
33 IC 5135	97	$> 10^4(e)$	70 NGC 4639	0.9	
34 NGC 3982	90		71 NGC 513	-	
35 NGC 3079	90	$160^{+270}_{-130}(a)$	72 NGC 4785	-	
36 NGC 5953	86		73 NGC 3362	-	
37 NGC 5899	74		74 NGC 7465	-	

$^{\dagger}[OIII]$  flux in units of  $10^{-14}$  erg s $^{-1}$  cm $^{-2}$ , corrected for the extinction as deduced from the (narrow line) Balmer decrement. No data are available for the last four sources.

$^{\ddagger}N_H$  in units of  $10^{20}$  cm $^{-2}$ .

\*Not corrected for the Balmer decrement.

\*\*Estimated (see text).

References: (a) B99, (b) Matt et al. (1999), (c) Risaliti et al. 1999, (d) Ueno private communication, (e) this work.

Table 2. Additional Sy2s from the Ho et al. sample.

Name	$F_{[OIII]}^{\dagger}$	$N_H^{\ddagger}$	Name	$F_{[OIII]}^{\dagger}$	$N_H^{\ddagger}$
1 NGC 3735	33	< 60 (a)	10 NGC 3976	2.4	
2 NGC 1167	17		11 NGC 4698	2.4	
3 NGC 2655	16		12 NGC 4725	2.1	
4 NGC 4565	6		13 NGC 3486	1.7	
5 NGC 3254	5		14 NGC 1058	1.3	
6 NGC 4477	4		15 NGC 4378	0.8	
7 NGC 3941	3		16 NGC 185	0.2	
8 NGC 4138	2.9		17 NGC4472	0.1	
9 NGC 676	2.9		18 NGC 4168	0.1	

$^{\dagger}[OIII]$  flux in units of  $10^{-14}$  erg s $^{-1}$  cm $^{-2}$ , corrected for the extinction as deduced from the (narrow line) Balmer decrement.

$^{\ddagger}N_H$  in units of  $10^{20}$  cm $^{-2}$ .

References: (a) this work

$\log(N_H)(\text{cm}^{-2})$	% Sy2s
$< 22$	$4.44 \pm 2.87$
22-23	$17.78 \pm 5.64$
23-24	$29.91 \pm 7.72$
24-25	$21.53 \pm 7.03$ (17.09)
$> 25$	$26.33 \pm 7.13$

Table 3: The numerical values corresponding to Figure 4.

## REFERENCES

- Antonucci, R.R.J. 1993, *ARA&A*, 31, 473
- Bassani, L., Dadina, M., Maiolino, R., et al. 1999, *ApJS*, in press (B99)
- Awaki, H. 1997, in “Emission Lines in Active Galaxies”, Peterson B.M., Cheng F.Z., Wilson A.S (eds.) *ASP Conference Series*, 113, p. 44
- Cagnoni, I., Della Ceca, R., and Maccacaro, T. 1998, *ApJ*, 493, 54
- Comastri, A., Setti, G., Zamorani, G., and Hasinger, G. 1995, *A&A*, 296, 1
- di Serego Alighieri, S., Cimatti, A., Fosbury, R.A.E., and Hes, R. 1997, *A&A*, 328, 510
- Gilli, R., Comastri, A., Brunetti, G., and Setti, G. 1999a, *New Astron.*, in press
- Gilli, R., Risaliti, G., Salvati, M. 1999b, *A&A*, submitted
- Giommi, P., Fiore, F., Ricci, D., Molendi, S., Maccarone, A., Comastri, A. 1998, in “The Active X-ray Sky: Results from BeppoSAX and Rossi-XTE”, L. Scarsi, H. Bradt, P. Giommi, F. Fiore (eds.), p. 591
- Granato, G.L., Danese, L., and Franceschini, A. 1997, *ApJ*, 486, 147
- Helfer, L. 1997, *Ap&SS* 248, 51
- Hes, R., Barthel, P.D., Fosbury, R.A.E. 1993, *Nature*, 362, 326
- Ho, L. C., Filippenko, V. and Sargent, W.L.W. 1997, *ApJS*, 112, 315
- Keel, W.C. 1980, *AJ*, 85, 198
- Maiolino, R., and Rieke, G.H. 1995, *ApJ*, 454,95 (MR)
- Maiolino, R., Salvati, M., Bassani, L., et al. 1998a, *A&A*, 338, 781 (M98)
- Maiolino, R., Krabbe, A., Thatte, N., Genzel, R. 1998b, *ApJ*, 493, 650
- Malkan, M.A., Gorjian V., and Tam R. 1998, *ApJS*, 117, 25
- Matt, G., Guainazzi, M., Maiolino R., et al. 1999, *A&A*, submitted
- Miyaji, T., Hasinger, G., and Schmidt, M. 1999, in “Highlights in X-ray Astronomy in Honor of Joachim Truemper’s 65th birthday”, in press
- Risaliti, G., Bassani, L., Comastri, A., et al. 1999 *Proceedings of the Third Italian Conference on AGNs, MemSAIt*, in press

- Salvati, M., Bassani, L., Dadina, M., Della Ceca, R., Matt, G., Maiolino, R. & Zamorani, G. 1997, *A&A*, 323, L1
- Sandage, A. and Tammann, G.A. 1987, “A revised Shapley-Ames catalog of bright galaxies”, Carnegie Institution of Washington Publication, Washington D.C.
- Simcoe, R., McLeod, K.K., Chachter, J., and Elvis, M. 1997, *ApJ*, 489, 615
- Thatte, N., Quirrenbach, A., Genzel, R., Maiolino, R., and Tecza, M. 1997, *ApJ*, 490, 238

**Figure captions:**

Fig. 1.— The absorbing  $N_H$  as a function of the (extinction corrected) [OIII] luminosity (upper panel) and of the absorption corrected 2–10 keV luminosity (lower panel) for the subsample of objects with  $F_{[OIII]} > 40 \times 10^{-14} \text{ cm}^{-2} \text{ erg s}^{-1}$ . There is no evidence of a correlation between the absorbing column density and the intrinsic luminosity of the AGN. In the lower panel we only plot objects whose X-ray spectra show the direct transmitted component, because it is not possible to estimate the intrinsic X-ray luminosity from the reflected component alone.

Fig. 2.— The axial ratio distribution for the sources with  $F_{[OIII]} > 40 \text{ erg cm}^{-2} \text{ s}^{-1}$  (upper histogram) and for the sources with  $F_{[OIII]} \leq 40 \text{ erg cm}^{-2} \text{ s}^{-1}$  (lower histogram). We have not included elliptical and S0 galaxies. The fainter subsample is clearly biased in favor of face-on systems.

Fig. 3.— The [OIII] flux distribution of the total sample (Tab. 1 plus Tab. 2). The shaded bars refer to the additional sources from Ho et al. (1997)

Fig. 4.— The column density distribution of our final subsample of 45 Seyfert 2 galaxies. The shaded part in the fourth bar indicates the sources for which only a lower limit of  $10^{24} \text{ cm}^{-2}$  is available at present.

Fig. 5.— The separate contribution to the  $N_H$  distribution from “strict” type 2 Seyferts (upper panel) and from intermediate type 1.8–1.9 Seyferts (lower panel).



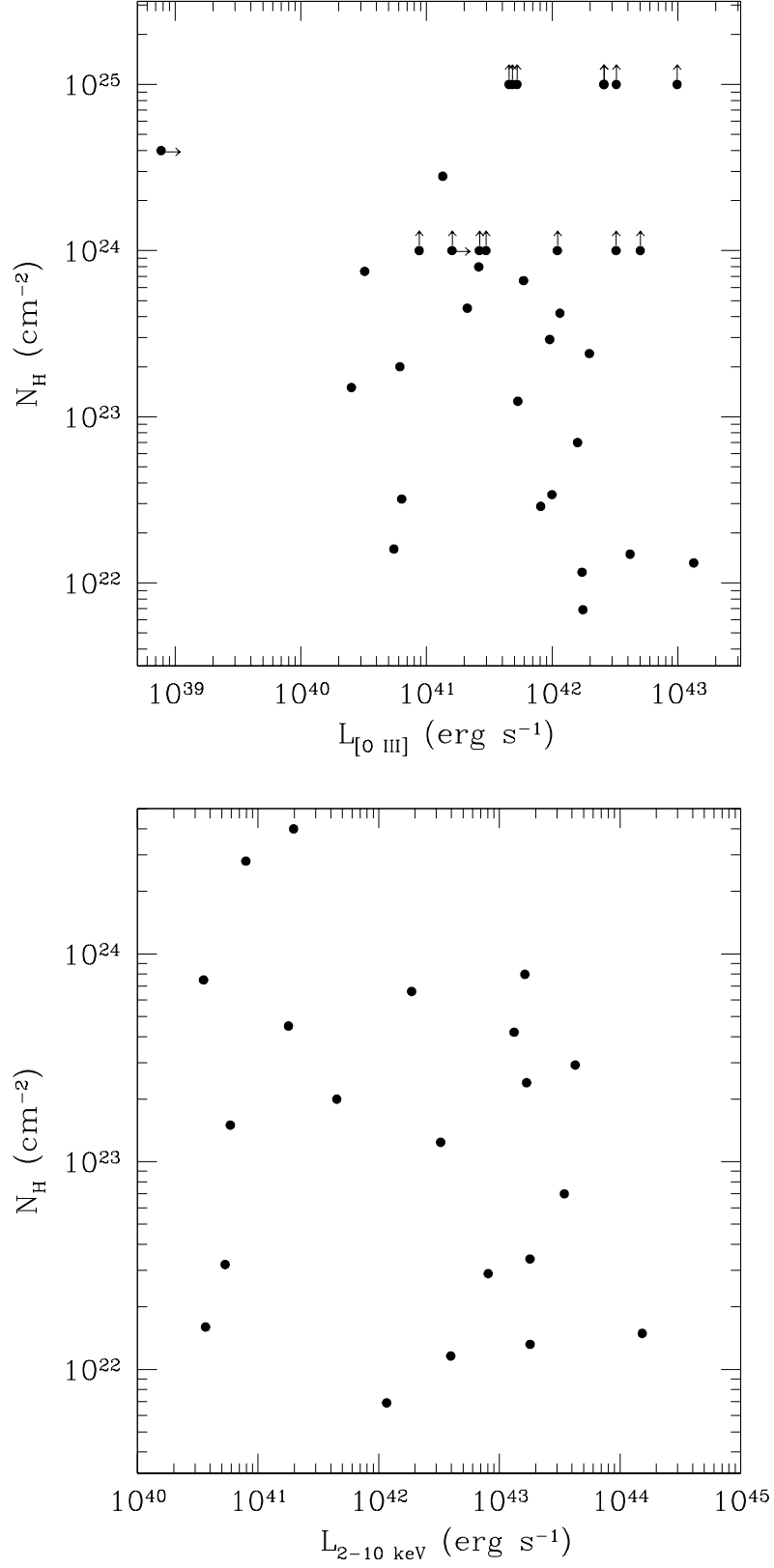


Fig. 1.—

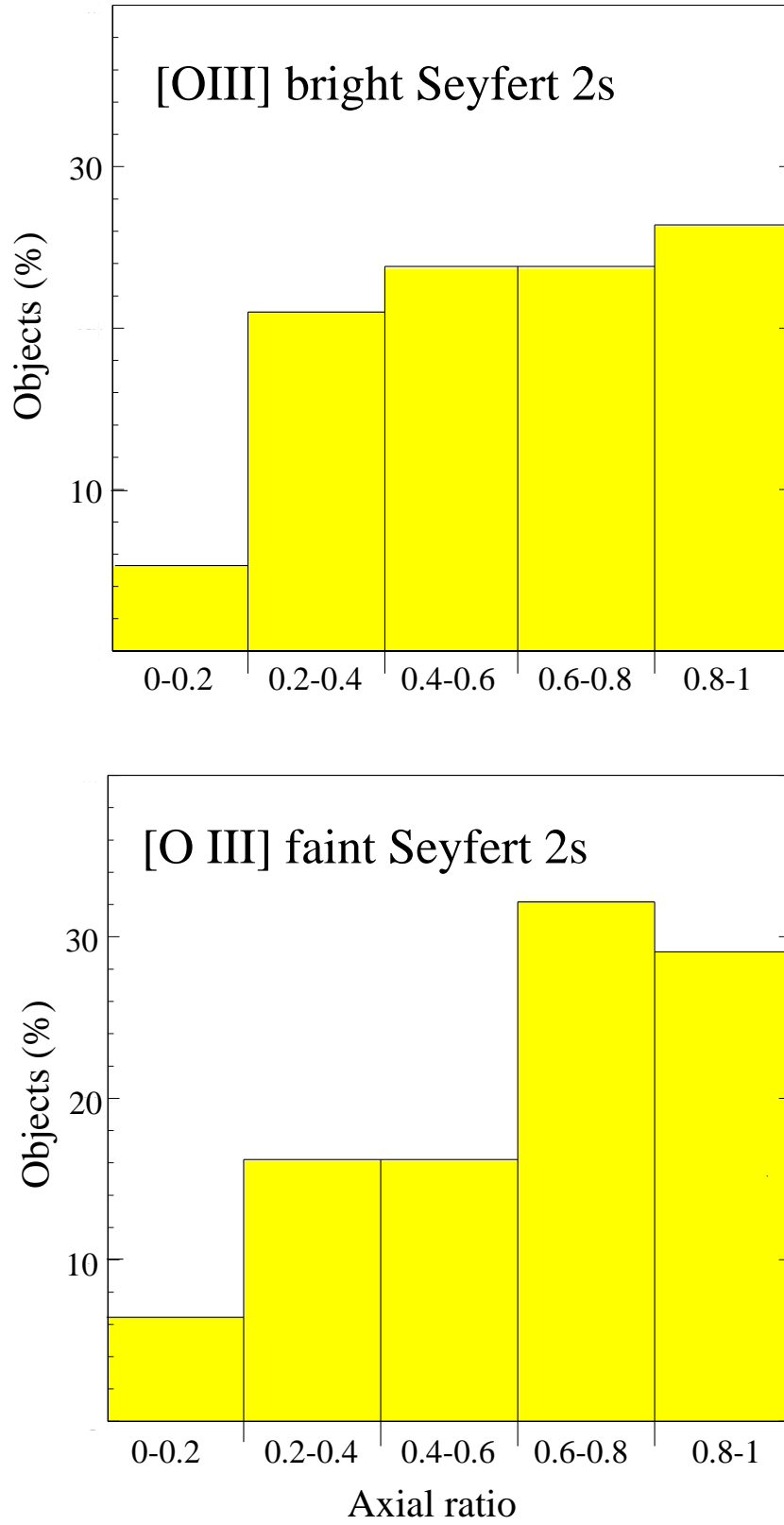


Fig. 2.—

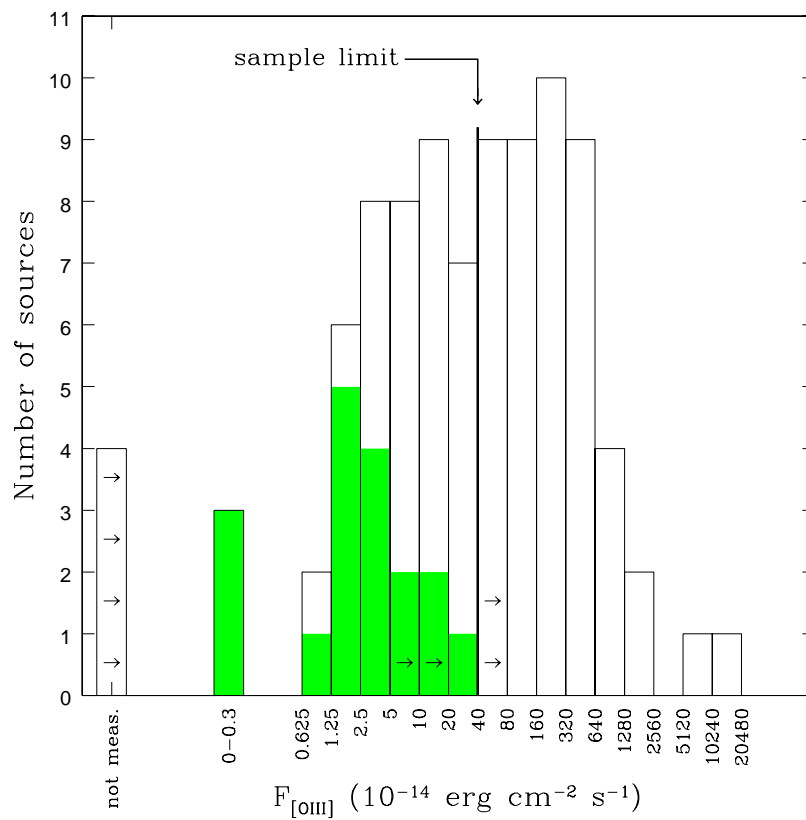


Fig. 3.—

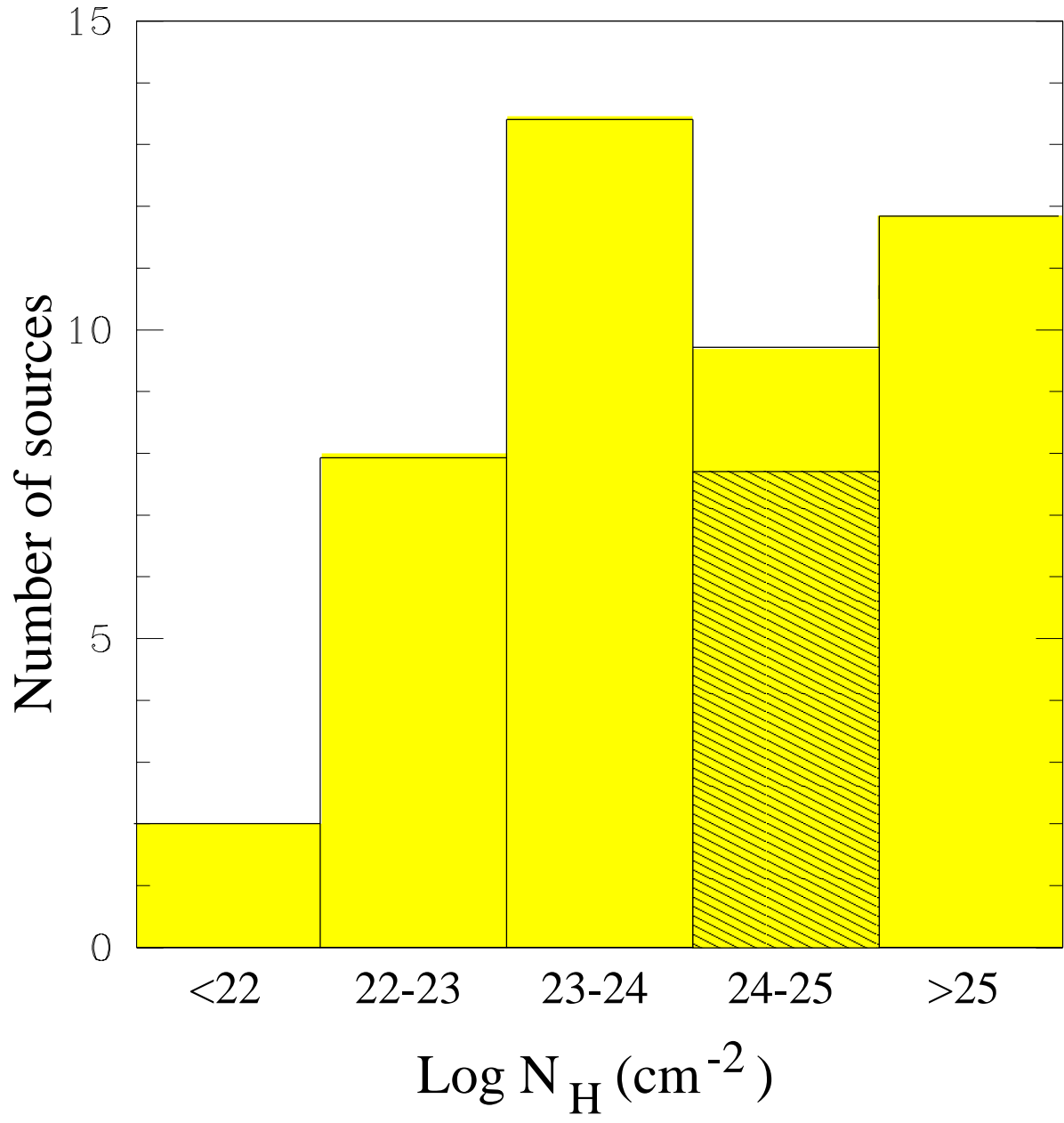


Fig. 4.—

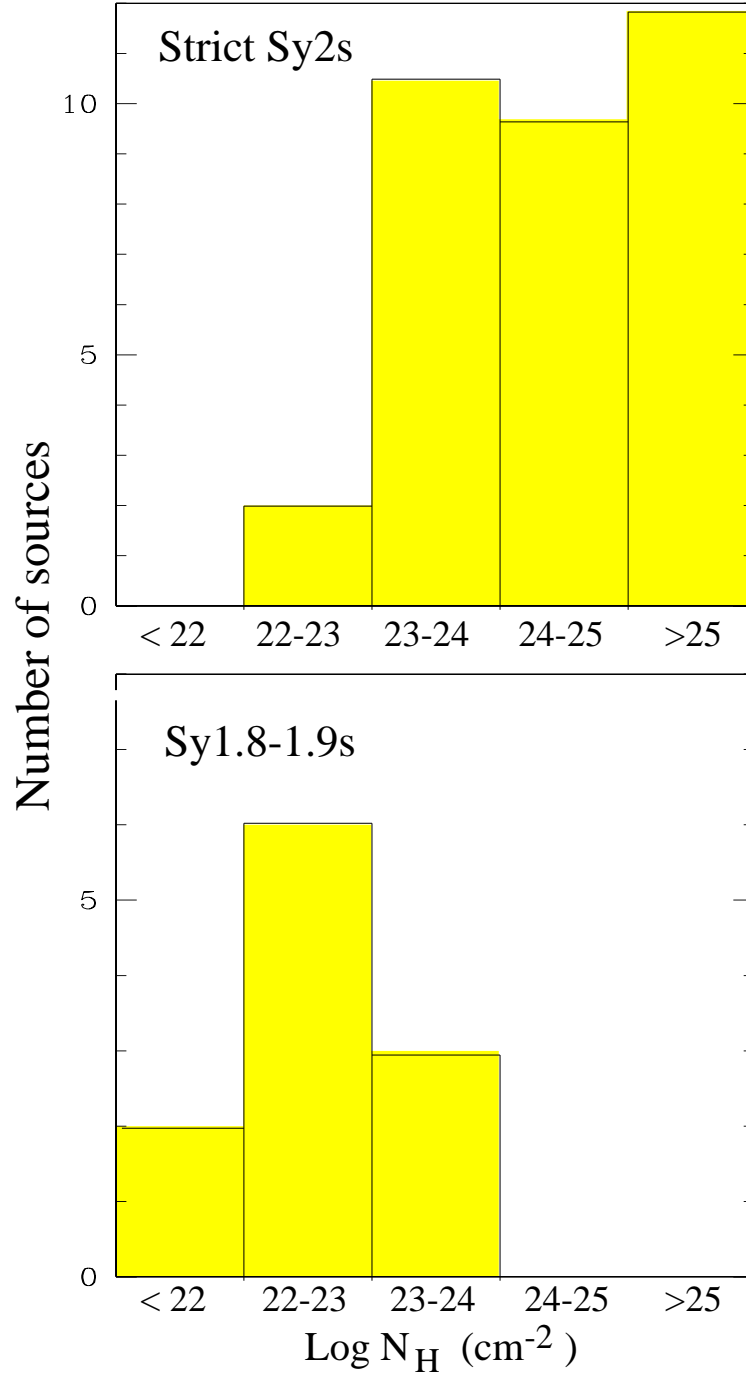


Fig. 5.—